JOURNAL OF SOLID STATE CHEMISTRY **59**, 60–64 (1985)

New Alkaline Earth Equiatomic Phases: SrAu and BaAu

M. L. FORNASINI

Istituto di Chimica Fisica, Università di Genova, Corso Europa,
Palazzo delle Scienze, 16132 Genoa, Italy

Received September 21, 1984; in revised form December 4, 1984

The phases SrAu and BaAu were synthesized and characterized structurally. SrAu, *mP*40, space group $P2_1/m$, a = 40.13(2), b = 4.697(1), c = 6.192(4) Å, β = 94.21(6)°, Z = 20, is a new stacking variant of the FeB–CrB type, with Jagodzinski notation hch_2ch_2chc. The structure was refined from single crystal diffractometric data with R = 0.090. BaAu, *oP*8, space group *Pnma*, a = 8.338(5), b = 4.925(1), c = 6.390(4) Å, Z = 4, crystallizes in the FeB structure type. A general correlation among the *AB* equiatomic phases formed by the alkaline earths with VIII to IVB group elements is found by reporting the *B–B* chain angle against the combination $R_\sigma^{AB} = |(r_s^A + r_p^A) - (r_s^B + r_p^B)|$ with Zunger's r orbital radii. © 1985 Academic Press, Inc.

Introduction

Several alkaline earth equiatomic compounds with IB and IIB elements have been studied in recent years (*1–4*). Most of them crystallize in the FeB structure type, like BaAg and SrZn; in the Cr*B* type, like CaAg, CaAu and CaZn; or in a stacking variant of the Fe*B*–Cr*B* type, like α- and β-CaCu and SrAg. Two others have a different structure of their own: SrCu and BaCu. In all cases, alkaline earth trigonal prisms around the second element are a common feature relating these structures.

Two phases remain undetermined: SrAu and BaAu. A phase near the equiatomic composition with congruent melting point at ~1243 K is present in the system Sr–Au (*5*), while for the system Ba–Au no data are available. This work concerns the identification and structural characterization of these two phases.

Experimental

Stoichiometric amounts of Ba (99.5% pure, Fluka, Buchs, Switzerland) or Sr and Au (99.0% and 99.999% pure, Koch–Light, Coinbrook, England) were placed in tantalum containers and sealed under argon. After melting, SrAu was further annealed for 2 months at 923 K. The alloys were brittle and well crystallized but their high oxidizability prevented the usual metallographic check for homogeneity to be applied.

The two compounds were examined by both single crystal and powder methods. Precession patterns of several SrAu crystals always showed monoclinic symmetry with 0*k*0 reflections present only for $k = 2n$, indicating $P2_1$ and $P2_1/m$ as possible space groups, and an intensity distribution typical of a stacking variant of the Fe*B*–Cr*B* type.

A single crystal of SrAu measuring 0.03 × 0.08 × 0.10 mm was mounted on an

0022-4596/85 $3.00

Enraf–Nonius CAD-4 automatic diffractometer with graphite-monochromated Mo$K\alpha$ radiation ($\lambda = 0.71069$ Å). Reflections in a hemisphere of the reciprocal lattice were collected with the ω scan mode in the range $6 \leq 2\vartheta \leq 54°$, yielding 2975 averaged independent reflections. The intensity data were processed for Lp and absorption effects ($\mu = 88.5$ mm^{-1}) applying both the correction for spherical crystals and a semiempirical correction based on the azimuthal scan of a top reflection. The ratio between the maximum and minimum transmission factor was 9.5. The lattice constants were determined by least squares from 25 diffractometer-measured high-angle reflections: $a = 40.13(2)$, $b = 4.697(1)$, $c = 6.192(4)$ Å, $\beta = 94.21(6)°$. Refinement of the proposed model was made with SHELX 76 (*6*), taking scattering and anomalous dispersion factors from (*7*).

Several BaAu crystals were mounted on the diffractometer, but none could be used for data collection as they decomposed after a short time. However, it was possible to establish orthorhombic symmetry with $0kl$ reflections present only for $k + l = 2n$ and $hk0$ present only for $h = 2n$, indicating $Pn2_1a$ and $Pnma$ as possible space groups, and derive the lattice constants values $a = 8.338(5)$, $b = 4.925(1)$, $c = 6.390(4)$ Å.

Results

Following the indications given by Klepp and Parthé (*8*, *9*) 14 stacking variants of the Fe*B*–Cr*B* type consistent with the observed lattice constants were tried as starting models for the structure of SrAu. One of these in the space group $P2_1/m$ gave a satifactory agreement and was isotropically refined (61 parameters, 949 reflections with $F_o > 2\sigma(F_o)$, unit weights) with a final conventional R of 0.090. The relatively high value of the residual can be ascribed both to severe absorption correction and to a probable degree of disorder in a stacking of such a long period.

TABLE I

ATOMIC COORDINATES AND ISOTROPIC THERMAL PARAMETERS OF SrAu (SPACE GROUP $P2_1/m$)

	x	z	U (Å^2)
Sr(1)	0.0162(5)	0.765(3)	0.015(4)
Sr(2)	0.1135(4)	0.566(3)	0.008(3)
Sr(3)	0.2143(5)	0.858(3)	0.015(4)
Sr(4)	0.3137(5)	0.653(3)	0.011(3)
Sr(5)	0.4150(5)	0.485(3)	0.013(3)
Sr(6)	0.5149(4)	0.761(3)	0.008(3)
Sr(7)	0.6149(4)	0.031(3)	0.011(3)
Sr(8)	0.7142(4)	0.847(3)	0.009(3)
Sr(9)	0.8124(5)	0.649(3)	0.015(4)
Sr(10)	0.9131(5)	0.947(3)	0.014(4)
Au(1)	0.0412(3)	0.284(2)	0.026(2)
Au(2)	0.1437(2)	0.081(1)	0.006(1)
Au(3)	0.2433(2)	0.373(1)	0.011(2)
Au(4)	0.3420(2)	0.162(1)	0.007(2)
Au(5)	0.4419(2)	0.999(1)	0.013(2)
Au(6)	0.5401(2)	0.274(1)	0.012(1)
Au(7)	0.6412(2)	0.553(1)	0.012(2)
Au(8)	0.7428(2)	0.369(1)	0.006(2)
Au(9)	0.8419(2)	0.153(1)	0.021(2)
Au(10)	0.9442(2)	0.457(1)	0.009(2)

Note. All atoms in equipoint $2(e)$ with $y = \frac{1}{4}$. The thermal factors are defined by $T = \exp[-8\pi^2 U(\sin\vartheta/\lambda)^2]$.

Atomic coordinates and isotropic thermal parameters of SrAu are reported in Table I (a list of observed and calculated structure factors can be obtained from the author on request).

In the case of BaAu, symmetry, extinctions, and lattice constants led us to propose the Fe*B* type as possible structure, and the model was confirmed using the parameters of the phase BaAg (*3*), by comparison of powder intensities observed on Debye–Scherrer photographs and values calculated with the program LAZY PULVERIX (*10*).

Discussion

A projection of the structure of SrAu

along the unique axis is drawn in Fig. 1 with the Sr trigonal prisms surrounding the Au atoms indicated. It represents a new stacking variant of the Fe*B*–Cr*B* type, resulting from the arrangement in the *a* direction of trigonal prisms alternately inclined as in the Fe*B* type or aligned as in the Cr*B* type. Both sequence and length of the fragments characterize each stacking and a complete description can be obtained using the codes proposed by Klepp and Parthé (*8, 9*). For SrAu they are: *hch*$_2$*ch*$_2$*chc* as Jagondzinski notation, connected with the interpretation of trigonal-prism-based structures in terms of the microtwinning mechanism (*11*), and corresponding to 60% of hexagonal stacking; (2)*2*1(*2*)1*2* is Zhdanov symbol giving the sequence of iso-oriented prisms.

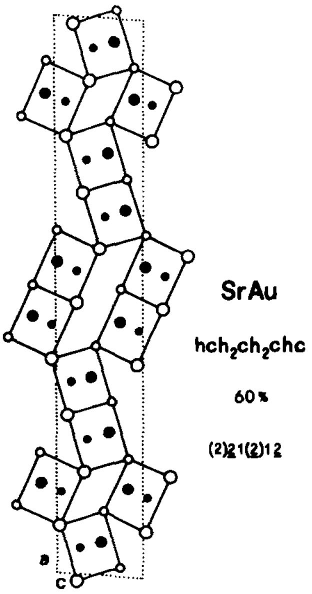

FIG. 1. Projection of the SrAu structure along the *b* axis. Open circles—Sr; full circles—Au. Small circles are at height ¼, large circles at height ¾.

TABLE II

INTERATOMIC DISTANCES AROUND THE AU ATOMS IN SrAu (Å)

Au(1)–2Au(10)	2.88(1)	Au(2)–2Au(9)	2.84(1)
– Sr(1)	3.21(2)	– Sr(3)	3.24(2)
– Sr(2)	3.27(2)	–2Sr(10)	3.27(2)
–2Sr(1)	3.29(2)	–2Sr(9)	3.31(1)
– Sr(1)	3.30(2)	– Sr(2)	3.32(2)
–2Sr(10)	3.36(2)	– Sr(2)	3.33(2)
Au(3)–2Au(8)	2.87(1)	Au(4)–2Au(7)	2.98(1)
– Sr(4)	3.20(2)	–2Sr(7)	3.20(1)
–2Sr(9)	3.24(1)	–2Sr(8)	3.25(1)
–2Sr(8)	3.26(1)	– Sr(4)	3.27(2)
– Sr(3)	3.30(2)	– Sr(4)	3.32(2)
– Sr(3)	3.31(2)	– Sr(5)	3.42(2)
Au(5)–2Au(6)	3.01(1)	Au(6)–2Au(5)	3.01(1)
–2Sr(6)	3.22(1)	–2Sr(6)	3.22(1)
–2Sr(7)	3.27(1)	– Sr(6)	3.25(2)
– Sr(5)	3.27(2)	–2Sr(5)	3.25(1)
– Sr(5)	3.28(2)	– Sr(6)	3.26(2)
– Sr(6)	3.37(2)	– Sr(7)	3.46(2)
Au(7)–2Au(4)	2.98(1)	Au(8)–2Au(3)	2.87(1)
– Sr(7)	3.21(2)	– Sr(9)	3.18(2)
–2Sr(5)	3.25(2)	– Sr(8)	3.25(2)
–2Sr(4)	3.28(1)	–2Sr(4)	3.26(2)
– Sr(7)	3.33(2)	–2Sr(3)	3.29(1)
– Sr(8)	3.33(2)	– Sr(8)	3.35(2)
Au(9)–2Au(2)	2.84(1)	Au(10)–2Au(1)	2.88(1)
– Sr(10)	3.21(2)	–2Sr(1)	3.20(1)
–2Sr(3)	3.25(2)	–2Sr(2)	3.29(1)
– Sr(9)	3.26(2)	– Sr(10)	3.31(2)
–2Sr(2)	3.36(1)	– Sr(1)	3.34(2)
– Sr(9)	3.37(2)	– Sr(10)	3.36(2)

As in all stacking variants of this family, each Au atom is surrounded by a Sr trigonal prism; three other contacts with two Au and one Sr atom emerge from the lateral faces of the prism. As shown in Table II, the Au–Au distances range from 2.84 to 3.01 Å and the Au–Sr distances from 3.18 to 3.46 Å. The closest Sr–Sr bond is 3.98 Å (distances around the Sr atoms are omitted in the table for brevity).

With the structural identification of SrAu and BaAu a nearly complete survey of the *AB* compounds formed by alkaline earths with VIII, IB, IIB, IIIB, and IBV elements is now available and some general correlation can be tried. Most phases crystallize in the Fe*B* or Cr*B* type or in one of their stacking variants, where two types of interactions seem to be important: the *A*–*B* bond, giving rise to the characteristic trigonal prismatic coordination around the *B* atoms and regulating the shape of this polyhedron, and the *B*–*B* bond present in the infinite zigzag chains formed by the *B* elements and determining the amplitude of the chain angle.

Parthé and co-workers (*12–14*) divided the phases crystallizing in these structure types into two groups depending on the shape of the trigonal prisms. Application of the same criterion to equiatomic compounds formed by the divalent elements Ca, Sr, Ba, Eu, and Yb showed the occurrence of stretched prisms for B = Si, Ge, Sn, Pb and compressed prisms for B = Ni, Pd, Pt, Cu, Ag, Au (*4*). Another quantitative correlation was found by Chelikowsky and Phillips (*15*), namely a linear trend between the chain angle in alkaline earth Cr*B*-type compounds with Si, Ge, and Sn and the St. John-Bloch electronegativity difference. However, if we now insert in this graph the points corresponding to the equiatomic phases with Cu, Ag, Au, Zn, and Ga recently identified, we find that they are randomly distributed on both sides of the straight line passing through the points of the original plot.

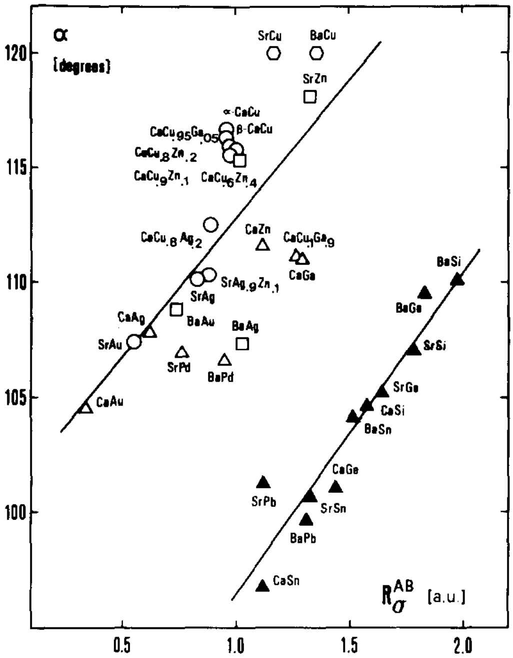

FIG. 2. Chain angle α formed by the partner elements in *AB* equiatomic compounds of alkaline earths, reported vs the orbital radii combination $R_\sigma^{AB} = |(r_s^A + r_p^A) - (r_s^B + r_p^B)|$. ▲—Cr*B* type with stretched prisms; △—Cr*B* type with compressed prisms; □—Fe*B* type; ○—stacking variants of the Fe*B*–Cr*B* type; ⬡—BaCu type.

The St. John–Bloch electronegativity is evaluated as sum of the reciprocal orbital radii r_l for $l = 0, 1, 2$ defined as the crossing points of the nonlocal pseudopotential. Recently two series of r_l values were derived, one from atomic spectral data (*16*) and the other from first principles (*17*), and their appropriate combinations were successfully used as dual coordinates in structural maps, to define regions where all examples of one structural type are found.

The chain angle in the alkaline earth phases has been plotted against each of these combinations. The best correlation is given by the parameter $R_\sigma^{AB} = |(r_s^A + r_p^A) - (r_s^B + r_p^B)|$ with Zunger's orbital radii (*17*), and is shown in Fig. 2. Here are reported the binary phases formed by VIII to IVB group elements together with some pseudobinary phases in the systems $CaCu_{1-x}Ag_x$, $CaCu_{1-x}Zn_x$, $CaCu_{1-x}Ga_x$, and $SrAg_{1-x}Zn_x$ (*18*). SrCu and BaCu are further adjoined, as the copper atoms are also surrounded by alkaline earth trigonal prisms and form graphite-like nets with bond angle always of 120° (*1*). All these phases correspond to different structure types: Fe*B*, Cr*B*, 9 stacking variants of the Fe*B*–Cr*B* type, and BaCu. In most cases the atomic parameters necessary to calculate the chain angle were available with a good precision from single crystals, otherwise from powder data; in some other cases they were reasonably assigned, as BaAu (parameters of BaAg), SrPd and BaPd (parameter of CaAg), and CaGa (parameter of $CaCu_{0.1}Ga_{0.9}$). In the stacking variants, where more than one position for the B atoms are present, a mean value of the chain angle is reported. A mean value is also used when more authors refined parameters of the same compound (*19, 20*). Although no estimated errors are given in the graph for the sake of clarity, nevertheless the uncertainty in the angle can be evaluated ±1°.

One observes in Fig. 2 that R_{σ}^{AB} provides a natural separation of the phases into two groups corresponding to the presence of stretched and compressed trigonal prisms, respectively. Moreover, the CrB-type phases formed by Si, Ge, Sn, and Pb maintain a good linear trend, analogous to that of the plot of Chelikowsky and Phillips, whereas the phases formed by Pd, Cu, Ag, Au, Zn, and Ga also have a certain tendency to a linear trend, even if some scatter in the points is recognizable.

It has to be remarked that the points of the first set, showing a good linear trend, belong to binary phases with elements of the same group (IVB) and with the same structure type (CrB), while points of the second set correspond to binary and pseudobinary phases with elements of four groups (VIII, IB, IIB, and IIIB) crystallizing in 12 structural types. Therefore, with all this in mind and also taking into account the strong dependence of the chain angle on a small variation of the atomic parameters, the observed trends remain significant.

In conclusion, the graph reflects a double capability of the orbital radii: on one hand they succeed in dividing the phases according to the trigonal prism shape; on the other hand they are able to produce a linear trend for phases with the IVB group elements, behaving as a kind of dimensional parameter.

Acknowledgment

The author thanks Professor A. Iandelli for his interest during the work.

References

1. M. L. Fornasini and F. Merlo, *Acta Crystallogr. B* **36,** 1288 (1980).
2. M. L. Fornasini, F. Merlo, and K. Schubert, *J. Less-Common Met.* **79,** 111 (1981).
3. F. Merlo and M. L. Fornasini, *Acta Crystallogr. B* **37,** 500 (1981).
4. F. Merlo, *J. Less-Common Met.* **86,** 241 (1982).
5. M. Feller-Kniepmaier and T. Heumann, *Z. Metallkd.* **51,** 404 (1960).
6. G. M. Sheldrick, "SHELX 76: A Program for Crystal Structure Determination," University of Cambridge, England, 1976.
7. "International Tables for X-Ray Crystallography," Vol. IV, p. 99, Kynoch Press, Birmingham, England (1974).
8. K. Klepp and E. Parthé, *Acta Crystallogr. B* **36,** 774 (1980).
9. K. Klepp and E. Parthé, *Acta Crystallogr. A* **37,** 61 (1981).
10. K. Yvon, W. Jeitschko, and E. Parthé, *J. Appl. Crystallogr.* **10,** 73 (1977).
11. E. Parthé, *Acta Crystallogr. B* **32,** 2813 (1976).
12. O. Schob and E. Parthé, *Acta Crystallogr.* **19,** 214 (1965).
13. D. Hohnke and E. Parthé, *Acta Crystallogr.* **20,** 572 (1966).
14. E. Parthé, *in* "Structure and Bonding in Crystals" (M. O'Keeffe and A. Navrotsky, Eds.), Vol. II, p. 259, Academic Press, New York, 1981.
15. J. R. Chelikowsky and J. C. Phillips, *Phys. Rev. B* **17,** 2453 (1978).
16. A. N. Bloch and G. C. Schatteman, *in* "Structure and Bonding in Crystals" (M. O'Keeffe and A. Navrotsky, Eds.), Vol. I, p. 49, Academic Press, New York, 1981.
17. A. Zunger, *in* "Structure and Bonding in Crystals" (M. O'Keeffe and A. Navrotsky, Eds.), Vol. I, p. 73, Academic Press, New York, 1981.
18. F. Merlo and M. L. Fornasini, *J. Less-Common Met.*, in press.
19. W. Rieger and E. Parthé, *Acta Crystallogr.* **22,** 919 (1967).
20. F. Merlo and M. L. Fornasini, *J. Less-Common Met.* **13,** 603 (1967).